A boundary element model of vascular gas bubble sticking and sliding

B. Eshpuniyani & J. L. Bull
Department of Biomedical Engineering, University of Michigan, U.S.A.

Abstract

A two dimensional channel flow in which a bubble adheres to one of the walls is studied computationally. The flow regime of interest here corresponds to very low Reynolds numbers. This allows us to model the flow using Stokes equations. The numerical method used is the boundary element method (BEM). A Tanner law is used to model the moving contact line dynamics. Both hydrophilic and hydrophobic channel walls are considered. The evolution of the bubble interface, pressure and velocity fields, and wall normal and shear stresses are studied for different values of inlet to outlet pressure ratios. The wall normal and shear stresses peak at the contact lines. It is shown that the horizontal force acting on the bubble approaches a constant value as the simulation progresses in time.

1 Introduction

A two dimensional channel flow in which a bubble adheres to one of the walls is studied computationally. This study is a part of an investigation into using a gas embolotherapy based technique for cancer treatment. This potential treatment modality uses gas bubbles to occlude blood flow to a tumor, thereby inducing tumor necrosis. The bubbles originate as perfluorocarbon droplets that are small enough to pass through capillaries. Low intensity ultrasound is used to track their motion. At the desired location the bubbles are vaporized using high intensity ultrasound to produce gas bubbles which are several times larger than the initial droplet size ([1, 2, 3, 4, 5, 6, 7]). These bubbles then stick in the vasculature, occluding the flow. The bubble sticking process likely involves the bubble contacting the vessel wall and then either sticking immediately or sliding some distance before becoming stuck or detaching from the wall. The effectiveness of the technique depends on where the bubbles stick and how much of the flow they occlude. In addition to

this principal motivation for the current study, there are many other scenarios in which a study of bubble dynamics in the cardiovascular system becomes important ([6]).

This study investigates the immobilization of the bubbles in the microcirculation, and the stresses imparted to the endothelium. A range of flow conditions are investigated to assess the likelihood of bubble sliding and the resulting wall shear and normal stresses.

2 Governing equations

We consider a bubble sticking in the microcirculation. The microcirculation regime is characterised by very small Reynolds numbers. This allows us to model the blood phase as an incompressible Stokes flow. The non-dimensional governing equations can written as

$$\nabla . \overrightarrow{u} = 0 \tag{1}$$

$$-\nabla p + \nabla^2 \overrightarrow{u} + Bo \overrightarrow{e}_g = 0 \tag{2}$$

The scaling used for this non-dimensionalization is $u^* = Uu$, $x^* = ax$, $p^* = \gamma p/a$ and $t^* = at/U$, where γ = surface tension, μ = liquid viscosity, a = half height of channel and $U = \gamma/\mu$. $Bo = \rho g a^2/\gamma$ is the Bond number and $\overrightarrow{e}_g$ is the unit vector in the direction of gravity.

3 Numerical method

The boundary element method (BEM) ([8], [9] and [10]) is used to solve the above governing equations. This method is based on the fact that the solution of linear, elliptic, homogeneous, partial differential equations can be represented by boundary integrals that involve the unknown function and its derivatives. For two-dimensional Stokes flow we have

$$\begin{aligned} c_{kj} u_k(\overrightarrow{x}_0) = &-\frac{1}{4\pi Ca} \int_C f_i(\overrightarrow{x}, \overrightarrow{x}_0) G_{ij}(\overrightarrow{x}, \overrightarrow{x}_0) dl(\overrightarrow{x}) \\ &+ \frac{1}{4\pi} \int_C u_i(\overrightarrow{x}) T_{ijk}(\overrightarrow{x}, \overrightarrow{x}_0) n_k(\overrightarrow{x}) dl(\overrightarrow{x}) \end{aligned} \tag{3}$$

where C is the selected boundary, $\overrightarrow{f} = \sigma . \overrightarrow{n}$ is the modified stress, $\sigma = (-p - Bo \overrightarrow{e}_g . \overrightarrow{x})I + Ca(\nabla \overrightarrow{u} + [\nabla \overrightarrow{u}]^T)$ is the modified stress tensor, $\overrightarrow{n}$ is the normal pointing into the domain, and c_{kj} is the tensor due to stress jump at the boundaries ($= \delta_{kj}/2$ for smooth boundaries). G_{ij} is a two dimensional Stokeslet defined as

$$G_{ij} = -\delta_{ij} ln|\overrightarrow{x} - \overrightarrow{x}_0| + \frac{(\overrightarrow{x}_i - \overrightarrow{x}_{0i})(\overrightarrow{x}_j - \overrightarrow{x}_{0j})}{(\overrightarrow{x} - \overrightarrow{x}_0)^2} \tag{4}$$

and T_{ijk} is the associated stress field defined as

$$T_{ijk} = -4 \frac{(\overrightarrow{x}_i - \overrightarrow{x}_{0i})(\overrightarrow{x}_j - \overrightarrow{x}_{0j})(\overrightarrow{x}_k - \overrightarrow{x}_{0k})}{(\overrightarrow{x} - \overrightarrow{x}_0)^4} \tag{5}$$

Quadratic elements are used to compute the integrals while solving (3) and cubic splines are used to compute the interface curvature.

4 Initial and boundary conditions

The simulations start with a semi-circular bubble attached to the lower wall of the channel. An initial bubble pressure is specified. In real life we could expect a bubble travelling through the vasculature to collide against the vessel wall, and stick with an interface shape and bubble pressure that would depend on the state of the bubble just before the impact. As the simulation progresses in time, the bubble shape and volume change. The ideal gas law is used to calculate the new bubble pressure at each time step. On the upper channel wall the no-slip and no penetration boundary condition is used. The lower wall requires special attention as we have two contact lines. The contact line velocity is computed using a Tanner's law ([11]) as follows

$$u_{cl} = k(\theta_D - \theta_S) \tag{6}$$

where θ_D is the dynamic contact angle between the bubble surface and channel wall at the contact line, while θ_S is the static contact angle. The velocity then decreases linearly with position as we move away from the contact line until reaching zero to avoid singularities at the contact lines. The values of k and θ_S will depend on the properties of the two fluids and the solid surface. The stress boundary condition, $\triangle \overrightarrow{f} = \kappa \overrightarrow{n}$, is used at the interface, where κ is the curvature of the interface. The kinematic boundary condition, $\frac{\partial \overrightarrow{Y}}{\partial t}.\overrightarrow{n} = \overrightarrow{u}.\overrightarrow{n}$ is used to advance the interface shape in time using Gear's method. The kinematic boundary condition simply implies that at any given point, the interface $(\overrightarrow{Y})$ moves at the local velocity $(\overrightarrow{u})$. Pressure is specified at the inlet and outlet to drive the flow.

5 Results and discussion

Figures 1 and 2 present the results for a hydrophilic surface. The static contact angle is set to 45^0. The value of k in the Tanner law is set to 0.1. First the evolution of the bubble when the inlet and outlet are maintained at the same pressure (set to 1) is studied. We see that both the contact lines move inwards (figure 1(a)) and the contact angle approaches the static value of 45^0. A stagnation point is formed at the center of the top channel wall. Peaks in the normal and shear wall stresses on the lower channel wall are observed at the contact lines (see figure 1(b)). The normal stress profile on the upper wall shows a bulge above the expanding bubble (this also corresponds to the stagnation region). The expansion of the bubble drives the flow out from both ends of the channel initially (see figure 1(c)) and the flow rates approach zero as the simulation progresses. Since the flow is symmetric in this case, the horizontal force on the bubble is nearly zero throughout the simulation (figure 1(d)).

Next we look at the flowfield and bubble evolution corresponding to p(in)/p(out) = 4, while keeping all other conditions the same as in case 1. We now have a

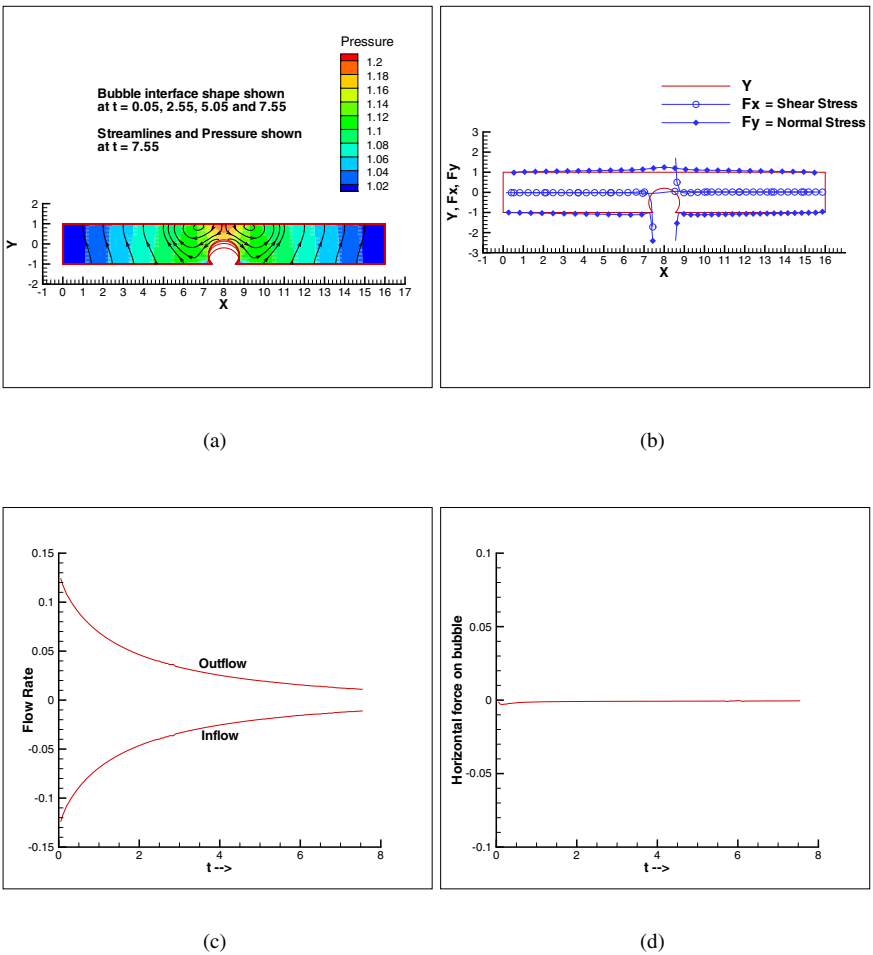

(a) (b)

(c) (d)

Figure 1: Static contact angle = 45^0, p(in)=p(out)=1, (a) Interface evolution, pressure contours and streamlines at t = 7.55, (b) Bubble shape, Wall normal and shear stresses at t = 7.55, (c) Flow rates at inlet and outlet, (d) Horizontal force on bubble.

pressure driven flow from left to right. The bubble leans into the flow (figure 2(a)). This reduces the contact angle at the front contact line. Hence the rear contact line has to move more than the front contact line for the contact angles to approach the static value of 45^0. Normal and shear wall stresses are plotted in figure 2(b). The normal wall stress on the upper channel wall shows a slight bulge above the expanding bubble. Both stresses show peaks at the contact lines on the lower wall. At the beginning of the simulation, the inlet has a flow rate that is less than the

outlet (figure 2(c)). This is due to the outward expansion of the bubble. The rapid motion of the bubble rear towards the right, and the leaning of the bubble into the flow, contribute to a sharp increase of the inlet flow rate. As the simulation progresses, both the inlet and outlet flow rate steadily approach a constant positive value. The horizontal force on the bubble approaches a constant value (figure 2(d)) as the simulation progresses in time.

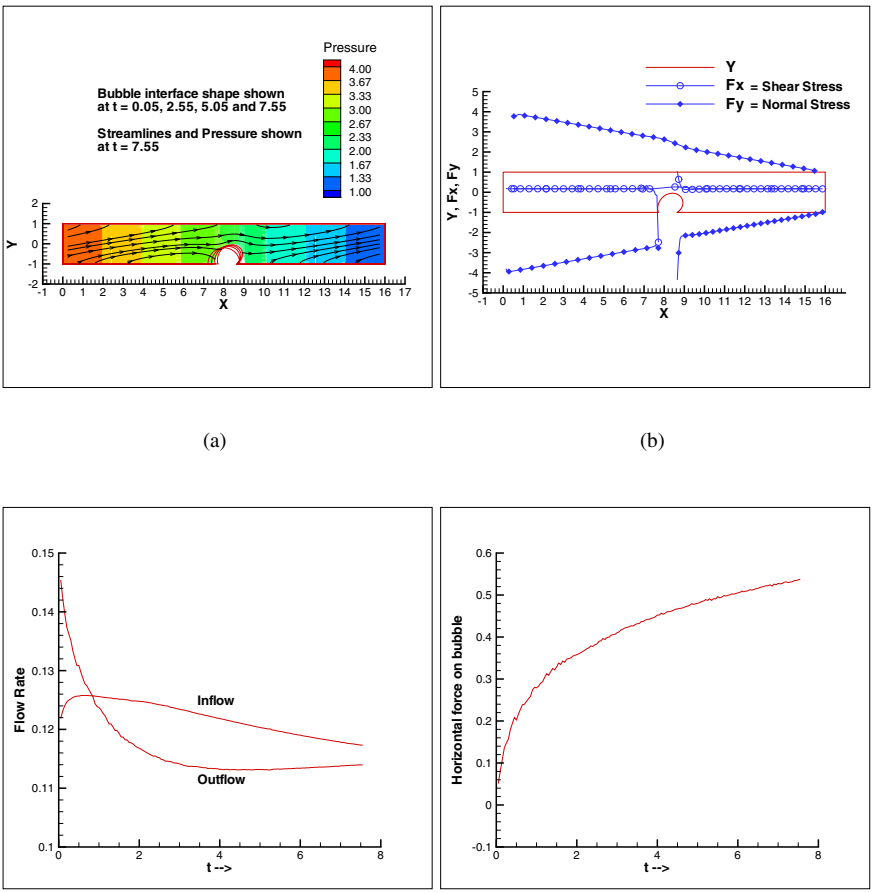

(a) (b)

(c) (d)

Figure 2: Static contact angle = 45^0, p(in)=4, p(out)=1,(a) Interface evolution, pressure contours and streamlines at t = 7.55, (b) Bubble shape, Wall normal and shear stresses at t = 7.55, (c) Flow rates at inlet and outlet, (d) Horizontal force on bubble.

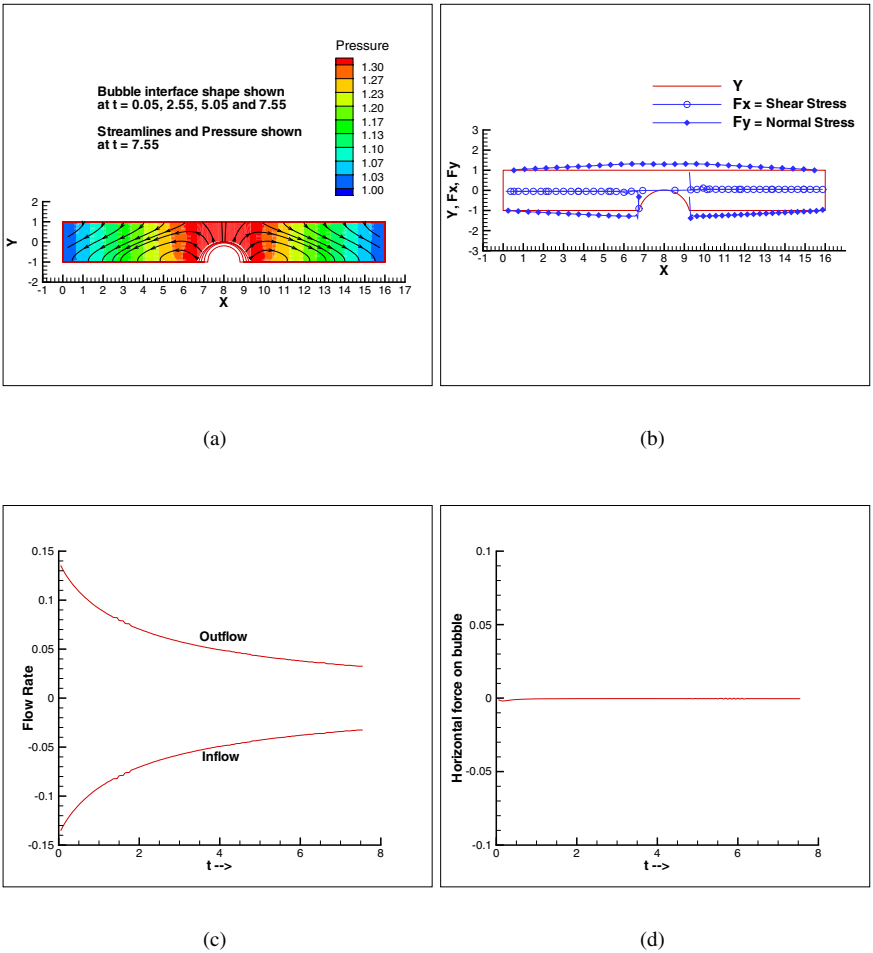

Figure 3: Static contact angle = 135^0, p(in)=p(out)=1,(a) Interface evolution, pressure contours and streamlines at t = 7.55, (b) Bubble shape, Wall normal and shear stresses at t = 7.55, (c) Flow rates at inlet and outlet, (d) Horizontal force on bubble.

Figures 3 and 4 present the results for a hydrophobic surface. The static contact angle is set to 135^0. The value of k in the Tanner law is set to 0.1. First the evolution of the bubble when the inlet and outlet are maintained at the same pressure (set to 1) is studied. Both the contact lines move outwards (figure 3(a)) and the contact angle approaches the static value of 135^0. A stagnation point is formed at the center of the top channel wall. Peaks in the normal and shear wall stresses on the lower channel wall are observed at the contact lines (see figure 3(b)). The normal

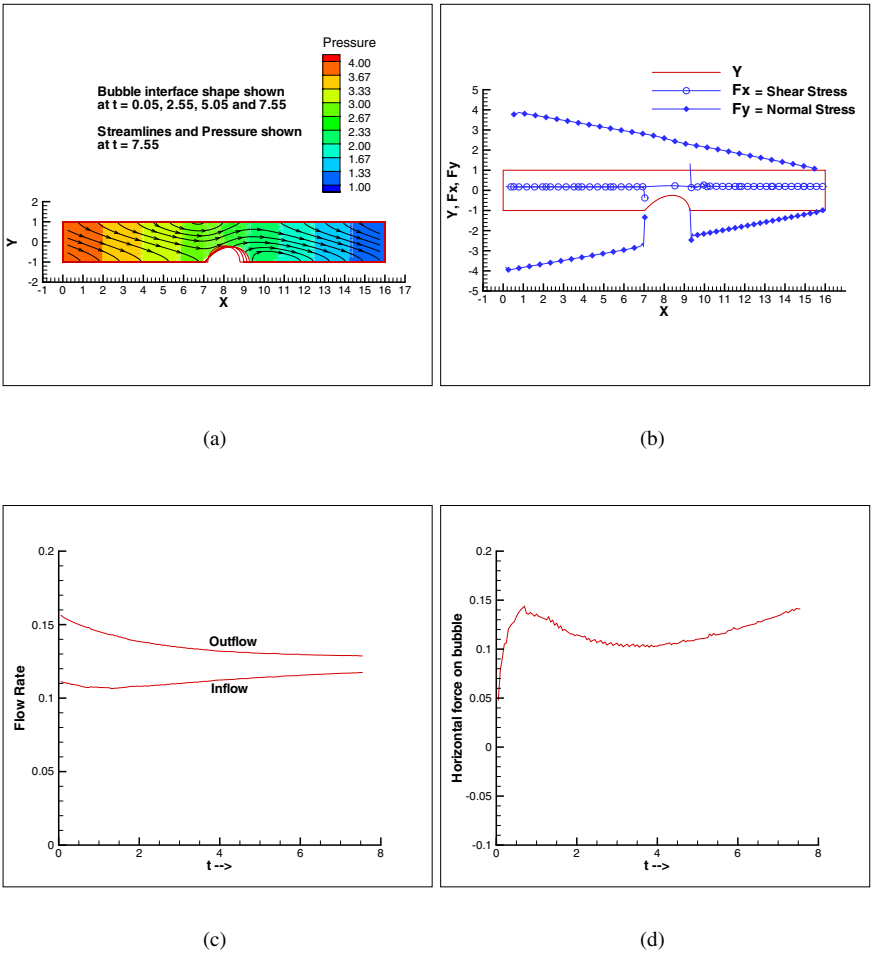

(a) (b)

(c) (d)

Figure 4: Static contact angle = 135^0, p(in)=4, p(out)=1,(a) Interface evolution, pressure contours and streamlines at t = 7.55, (b) Bubble shape, Wall normal and shear stresses at t = 7.55, (c) Flow rates at inlet and outlet, (d) Horizontal force on bubble.

stress profile on the upper wall shows a bulge above the expanding bubble. the expansion of the bubble drives the flow out from both ends of the channel initially (see figure 3(c)) and the flow rates approach zero as the simulation progresses. Since the flow is symmetric in this case, the horizontal force on the bubble is nearly zero throughout the simulation (figure 3(d)).

Next we look at the flowfield and bubble evolution corresponding to p(in)/p(out) = 4, while keeping all the other conditions same as in case 3. We now have a pres-

sure driven flow from left to right. We observe a flattening out of the bubble (figure 4(a)). The rear contact angle increases as the rear portion of the interface moves towards the wall. Hence the front contact line has to move more than the rear contact line for the contact angles to increase from their initial value and approach their static value of 135^0. The normal wall stress on the upper channel wall shows a slight dip above the bubble (see figure 4(b)). This is due to the progressive "flattening" of the bubble as the simulation progresses. Both stresses show peaks at the contact lines on the lower wall. At the beginning of the simulation, the inlet has a flow rate that is less than the outlet (figure 4(c)). This is again due to the outward expansion of the bubble. However we do not have a rapid motion of the bubble rear towards the right, and the leaning of the bubble into the flow. Thus no sharp increase of the inlet flow rate is observed. The outward motion of the contact lines (and hence the interface) result in a different time evolution of the inlet and outlet flow rates as compared to case 2. Whether the bubble will continue to slide along the channel wall, or eventually reach an equilibrium position, will depend on the relative magnitude of the horizontal force due to flow past the bubble (figure 4(d)), compared to the resistance from the surface tension and surface adhesion forces.

6 Conclusions

The boundary element method has been successfully implemented to study a 2-D pressure-driven channel flow with a bubble sticking and sliding along one of the channel walls. Contact lines are identified as high wall stress regions, which could potentially injure the underlying endothelium. This investigation demonstrates that the reduction in flow, the tendency of stuck bubbles to slide, and the bubble evolution depend on initial bubble pressure and wall surface properties. Understanding the biofluid mechanics of these bubbles will be essential to designing intelligent embolotherapy strategies. Future studies could consider a wider range of parameters and additional physiologic effects.

Acknowledgements

This work is supported by NIH Grant Number EB003541-01, NSF Grant Number BES-0301278, and Whitaker Foundation Grant Number RG-03-0017.

References

[1] Bull, J.L., Bubble transport in gas embolotherapy. *Faseb Journal*, **17(A144)**, 2003.
[2] Kripfgans, O.D., Fabiilli, M.L., Carson, P.L. & Fowlkes, J.B., On the acoustic vaporization of micrometer-sized droplets. *Journal of the Acoustical Society of America*, **116**, p. 272, 2004.
[3] Kripfgans, O.D., Fowlkes, J.B., Miller, D.L., Eldevik, O.P. & Carson, P.L.,

Acoustic droplet vaporization for therapeutic and diagnostic applications. *Ultrasound Med & Biol*, **26**, pp. 1177–1189, 2000.

[4] Kripfgans, O.D., Fowlkes, J.B., Woydt, M., Eldevik, O.P. & Carson, P.L., In vivi droplet vaporization for occlusion therapy and phase aberration correction. *IEEE Trans Ultrason Ferroelectr Freq Control*, **49**, pp. 726–738, 2002.

[5] Ye, T. & Bull, J.L., Direct numerical simulations of micro-bubble expansion in gas embolotherapy. *J Biomech Eng*, **126**, pp. 745–759, 2004.

[6] Bull, J.L., Cardiovascular bubble dynamics. *Critical Reviews in Biomedical Engineering*, **33(4)**, pp. 299–346, 2005.

[7] Calderon, A.J., Fowlkes, J.B. & Bull, J.L., Bubble splitting in bifurcating tubes: A model study of cardiovascular gas emboli transport. *J Appl Physiol*, **99**, 2005.

[8] Brebbia, C.A., *Boundary Elements: An Introductory Course*. UK: WIT Press, 1992.

[9] Bull, J.L., Hunt, A.J. & Meyhofer, E., A theoretical model of a molecular-motor-powered pump. *Biomedical Microdevices*, **7(1)**, pp. 21–33, 2005.

[10] Pozrikidis, C., *Boundary Integral and Singularity Methods for Linearized Viscous Flow*. Cambridge University Press: check, 1992.

[11] Greenspan, H.P., Motion of a small viscous droplet that wets a surface. *J Fluid Mech*, **84**, p. 125, 1978.